Reliable Non-Linear State Estimation involving Time Uncertainties

Simon Rohou[1], Luc Jaulin[1], Lyudmila Mihaylova[2], Fabrice Le Bars[1], Sandor M. Veres[2]

[1] ENSTA Bretagne, Lab-STICC, UMR CNRS 6285, Brest, France
[2] University of Sheffield, Sheffield, United Kingdom
simon.rohou@ensta-bretagne.org

***Abstract*—This paper presents an original approach for bounded-error state estimation involving time uncertainties. In this context, for a given bounded observation of the system, neither the value of the data nor the acquisition date are known exactly. We show that if the system is described by a continuous-time state equation, a constraint propagation approach allows to compute, for each t, a set enclosing all state vectors consistent with these measurements. The characterization is guaranteed even if the system is non-linear. Compared to other existing constraint approaches, the originality of our method is to enclose the set of all feasible trajectories inside a tube. This makes it possible to build specific operators for the propagation of time uncertainties through the whole trajectory. The efficiency of our approach is illustrated by two examples: the dynamic localization of a mobile robot and the correction of a drifting clock.**

***Index Terms*—time uncertainties, observations, tube programming, mobile robotics, constraints, contractors**

I. Introduction

This paper deals with the state estimation of a dynamical system of the form:

$$\left\{ \begin{array}{rcl} \dot{\mathbf{x}}(t) & = & \mathbf{f}(\mathbf{x}(t)), \\ y_j(t_j) & = & g(\mathbf{x}(t_j)), \end{array} \right. \tag{1}$$

where $\mathbf{x}(t) \in \mathbb{R}^n$ is the state vector representing the system at time t and $\mathbf{f} : \mathbb{R}^n \to \mathbb{R}^n$ a non-linear function depicting the evolution of the system. The observation function $g : \mathbb{R}^n \to \mathbb{R}$ is assumed to be scalar, without loss of generality. The $t_j, j \in \mathbb{N}$ are the measurement times and the y_j are the related outputs.

In a bounded-error approach, we can assume the function $\mathbf{f}$ and the measurements y_j are not known exactly. Instead, we shall consider that $\mathbf{f}$ is represented by a set-valued function $[\mathbf{f}]$ and that measurements y_j all belong to some known intervals denoted by $[y_j]$. When the t_j are exactly known, interval analysis [19] combined with constraint propagation [4, 12] is able to efficiently solve the state estimation problem [18, 13, 21]. More precisely, without any prior knowledge on the state, an interval approach allows to compute for each t a set enclosing all feasible state vectors.

This paper deals with uncertain measurement times: the t_j are only known to belong to some interval $[t_j]$. In this context, neither the value of the output y_i nor the acquisition date t_i are known exactly. Hence, the problem becomes much more difficult and the uncertainties related to the t_j are difficult to propagate through the differential equation. Some attempts using interval analysis have been proposed in [5, 3], but the corresponding observers cannot be considered as guaranteed. Other works, often referred as Out Of Sequence Measurement (OOSM) [9] state problems of time delay uncertainties, which can be somehow related to our problem. However, the considered time uncertainties are tight, in the order of algorithms time-step, and treated by means of covariance matrices which does not provide guaranteed results.

In contrast, this paper proposes a new reliable tool to deal with strong temporal uncertainty constraints. The contribution is designed to solve Constraint Satisfaction Problems (CSP) involving differential equations, non-linear functions and time uncertainties.

This paper is organized as follows. Section II gives an overview of constraint propagations related to sets of trajectories, introducing the concept of CSP, tubes and contractors. These tools will then be extended to the time uncertainty constraint this paper is dealing with. The approach, theoretically detailed in Section III, will be illustrated through two robotics examples. The first one, Section IV, involves a mobile robot to be localized while evolving between beacons emitting uncertain range-only signals. The second one, detailed in Section V, provides an original method to correct a drifting clock thanks to ephemeris measurements. Sections VI and VII conclude the paper and present the numerical libraries used during this work.

II. Constraint Propagation over Trajectories

Subsection II-A recalls the principle of constraint propagation [23, 4] that will be used later to formalize problems depicting dynamical systems. To this end, a *tube* can be used to enclose the domain of the feasible solution set: an envelope of trajectories compliant with the selected constraints. The notion of tube is recalled in Subsection II-B with related properties.

A. Constraint Satisfaction Problems

CSP. In numerical contexts, problems of control, state estimation and robotics can be described as *Constraint Satisfaction Problems* (CSP) in which variables must satisfy a set of rules or facts, called constraints, over domains defining a range of feasible values. Links between the constraints define a *Constraint Network* [16] involving variables $\{x_1, \ldots, x_n\}$, constraints $\{\mathcal{L}_1, \ldots, \mathcal{L}_m\}$ and domains $\{\mathbb{X}_1, \ldots, \mathbb{X}_n\}$ containing the x_i's. The variables x_i can be symbols, real numbers [1] or vectors of $\mathbb{R}^n$. The constraints can be non-linear equations between the variables, such as $x_3 = \cos(x_1 + \exp(x_2))$. Domains can be intervals, boxes [14], or polytopes [10, 24].

Contractors. A constraint $\mathcal{L}$ can be applied on a box $[\mathbf{x}] \in \mathbb{IR}^n$ with the help of a contractor $\mathcal{C}$. The box $[\mathbf{x}]$, also called *interval-vector*, is a closed and connected subset of $\mathbb{R}^n$ and belongs to the set of n-dimensional boxes denoted $\mathbb{IR}^n$. Formally, a contractor $\mathcal{C}$ associated to the constraint $\mathcal{L}$ is an operator $\mathbb{IR}^n \to \mathbb{IR}^n$ that returns a box $\mathcal{C}([\mathbf{x}]) \subseteq [\mathbf{x}]$ without removing any vector consistent with $\mathcal{L}$ [14, 8]. Constructing a store of contractors such as $\mathcal{C}_+$, $\mathcal{C}_{\sin}$, $\mathcal{C}_{\exp}$ associated to primitive equations such as $z = x+y$, $y = \sin(x)$, $y = \exp(x)$ has been the subject of much work.

Decomposition. Problems involving complex equations can be broken down into a set of primitive equations. Here, *primitive* means that the constraint cannot be decomposed anymore and that the related contractor is available in the collection of contractors, thus allowing to deal with a wide range of problems. For instance, the non-linear equation $x_3 = \cos(x_1 + \exp(x_2))$ can be decomposed into:

$$\left\{ \begin{array}{rcl} a & = & \exp(x_2), \\ b & = & x_1 + a, \\ x_3 & = & \cos(b). \end{array} \right. \tag{2}$$

Combining primitive contractors leads to a complex contractor that still provides reliable results [8].

Propagation. When working with finite domains, a propagation technique can be used to solve a problem. The process is run up to a fixed point when domains $\mathcal{D}$ cannot be reduced anymore.

Our goal is to consider trajectories as variables and to implement contractors to reduce their domains given a constraint that can be algebraic or differential. This will be done with the help of tubes that will be used as domains of these variables.

B. Tubes: envelopes of feasible trajectories

Definition. A tube is defined [15, 17] as an envelope enclosing an uncertain trajectory $\mathbf{x}(\cdot) : \mathbb{R} \to \mathbb{R}^n$. In this paper, we will use the definition given in [3, 6] where a tube $[\mathbf{x}](\cdot)$ is an interval of two trajectories $[\mathbf{x}^-(\cdot), \mathbf{x}^-(\cdot)]$ such that $\forall t,\ \mathbf{x}^-(t) \leqslant \mathbf{x}^+(t)$. A trajectory $\mathbf{x}(\cdot)$ belongs to the tube $[\mathbf{x}](\cdot)$ if $\forall t,\ \mathbf{x}(t) \in [\mathbf{x}](t)$. Figure 1 illustrates a tube enclosing a trajectory $x^*(\cdot)$.

Arithmetics on tubes. Consider two tubes $[x](\cdot)$ and $[y](\cdot)$ and an operator $\diamond \in \{+, -, \cdot, /\}$. We define $[x](\cdot) \diamond [y](\cdot)$ as the smallest tube (with respect to the inclusion) containing all feasible values for $x(\cdot) \diamond y(\cdot)$, assuming that $x(\cdot) \in [x](\cdot)$ and $y(\cdot) \in [y](\cdot)$. This definition is an extension to trajectories of the interval arithmetic proposed by Moore [20]. If f is an elementary function such as $\sin, \cos, \ldots$, we define $f\big([x](\cdot)\big)$ as the smallest tube containing all feasible values for $f\big(x(\cdot)\big)$, $x(\cdot) \in [x](\cdot)$.

Figures 2a–2b present two scalar tubes $[x](\cdot)$ and $[y](\cdot)$. The tube arithmetic makes it possible to compute any algebraic operation on tubes, as illustrated by Figures 2c–2f.

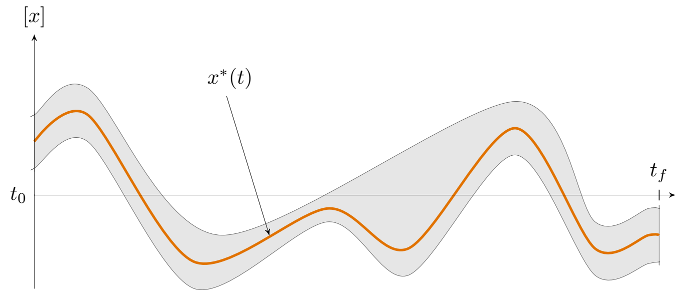

Fig. 1: A tube $[x](\cdot)$, interval of two functions $[x^-(\cdot), x^+(\cdot)]$, enclosing a random signal $x^*(\cdot)$.

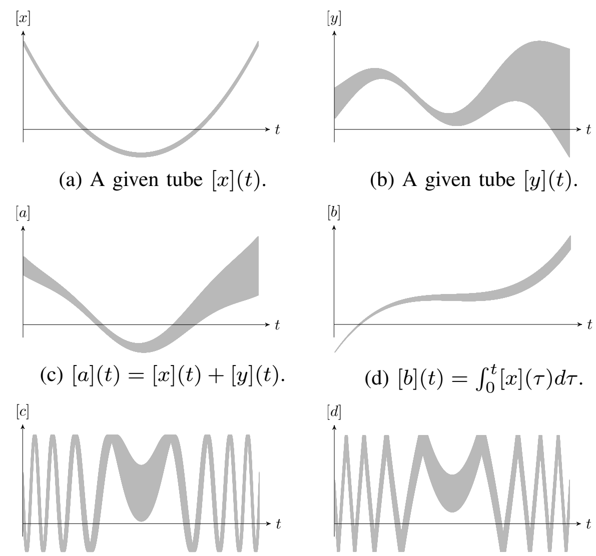

(a) A given tube $[x](t)$. (b) A given tube $[y](t)$.

(c) $[a](t) = [x](t) + [y](t)$. (d) $[b](t) = \int_0^t [x](\tau)d\tau$.

(e) $[c](t) = \sin([x](t))$. (f) $[d](t) = \arcsin([c](t))$.

Fig. 2: Tube arithmetics. Note that the vertical scales of these figures vary for full display.

Contractors for tubes. The contractors recalled in Subsection II-A can be applied on sets of trajectories, thus allowing constraints over time such as $a(t) = x(t) + y(t)$ or $b(t) = \sin(x(t))$. A *tube contractor* has been defined in [6] and is recalled here. A contractor applied on a tube $[a](\cdot)$ aims at removing unfeasible trajectories according to a given constraint $\mathcal{L}$:

$$[a](\cdot) \xrightarrow{\mathcal{C}_{\mathcal{L}}} [b](\cdot). \tag{3}$$

The output of the contractor $\mathcal{C}_{\mathcal{L}}$ is the tube $[b](\cdot)$ such that:

$$\forall t,\ [b](t) \subseteq [a](t), \qquad \text{(contraction)} \tag{4}$$

$$\left(\begin{array}{c} \mathcal{L}(a(\cdot)) \\ a(\cdot) \in [a](\cdot) \end{array} \right) \Longrightarrow a(\cdot) \in [b](\cdot). \quad \text{(completeness)} \tag{5}$$

For instance, the minimal contractor $\mathcal{C}_+$ associated with the constraint $a(\cdot) = x(\cdot) + y(\cdot)$, is:

$$\left(\begin{array}{c} [a](\cdot) \\ [x](\cdot) \\ [y](\cdot) \end{array} \right) \mapsto \left(\begin{array}{c} [a](\cdot) \cap ([x](\cdot) + [y](\cdot)) \\ [x](\cdot) \cap ([a](\cdot) - [y](\cdot)) \\ [y](\cdot) \cap ([a](\cdot) - [x](\cdot)) \end{array} \right). \tag{6}$$

In this way, information on either $[a](\cdot)$, $[x](\cdot)$ or $[y](\cdot)$ can be propagated to the other tubes. Figures 3a-3e picture

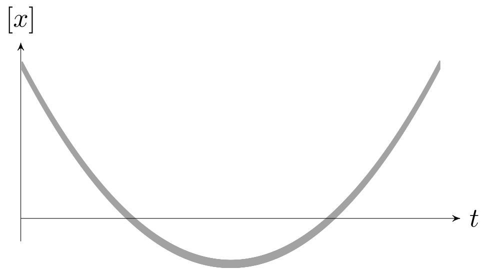

(a) Arbitrary envelope of feasible $x(\cdot)$.

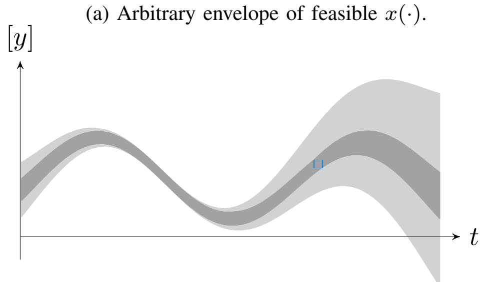

(b) Arbitrary contracted envelope of feasible $y(\cdot)$.

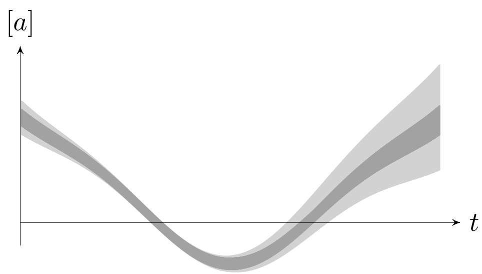

(c) Contracted envelope of feasible $a(\cdot) = x(\cdot) + y(\cdot)$.

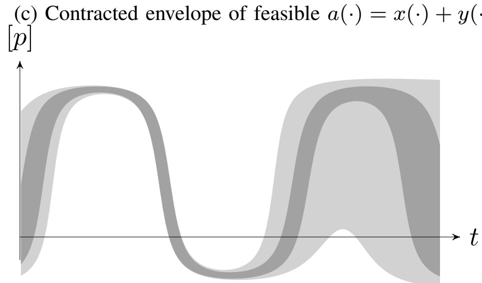

(d) Contracted envelope of feasible $p(\cdot) = \arctan(y(\cdot))$.

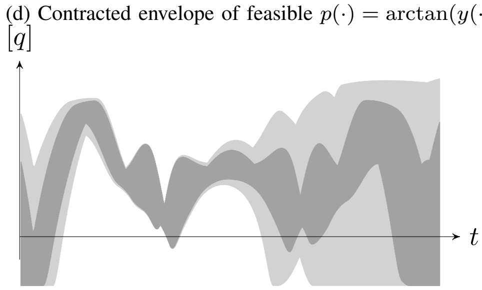

(e) Contracted envelope of feasible $q(\cdot) = 2\sin\left(\frac{a(\cdot)}{2}\right) + \sqrt{2p(\cdot)}$.

Fig. 3: Illustration of tubes contractions. Light gray areas represent the envelope of trajectories before contraction. Considering an improvement of the $y(\cdot)$ approximation, tubes $[a](\cdot)$, $[p](\cdot)$, $[q](\cdot)$ related to $[y](\cdot)$ by algebraic constraints can then be contracted. The final sets of solutions, obtained after applying contractors, is pictured in dark gray.

an improvement on a trajectory estimation towards related variables.

Differential contractor. The primitive constraint relying on the differential equation $\dot{x} = v$ has been the subject of [22], introducing the contractor $\mathcal{C}_{\frac{d}{dt}}([x](\cdot), [v](\cdot))$ defined by:

$$\begin{pmatrix} [x](t) \\ [v](t) \end{pmatrix} \mapsto \begin{pmatrix} \displaystyle\bigcap_{t_1=t_0}^{t_f} \left([x](t_1) + \int_{t_1}^{t} [v](\tau)d\tau\right) \\ [v](t) \end{pmatrix}, \quad (7)$$

where $[v](\cdot)$ encloses the set of feasible derivatives $\dot{x}(\cdot)$.

This contractor will be combined with the one that will be presented in Section III in order to propagate a local information over the whole domain of the set of feasible trajectories.

III. Dynamical Contractors involving Time Uncertainties

A trajectory observation can be seen as an elementary constraint in the field of CSP involving dynamical systems. This section provides a reliable tool to deal with a trajectory observation formalized by a primitive constraint denoted $\mathcal{L}_{\text{obs}}$. This will be formalized thanks to CSP, in which any uncertainty on the trajectory $x(\cdot)$, its evolution, the domain of observation $t \in \mathbb{R}$ or its value $y \in \mathbb{R}$ are bounded. Our contribution is to propose a new contractor that will optimally reduce these bounds by removing solutions not compliant with the considered constraint $\mathcal{L}_{\text{obs}}$.

In order to define the $\mathcal{L}_{\text{obs}}$ related contractor, new tubes properties have to be defined and are firstly provided below.

A. Tube properties involving domain uncertainties

Definition 1. The interval evaluation of a tube $[x](\cdot)$ over a bounded domain $[t]$ is given by [6]:

$$[x]([t]) = \bigsqcup_{t \in [t]} [x](t), \quad (8)$$

so that $[x]([t])$ is the smallest box enclosing all solutions for $x(t)$ such that $x(\cdot) \in [x](\cdot), t \in [t]$.

Definition 2. The tube set-inversion, denoted $[x]^{-1}([y])$, is defined by:

$$[x]^{-1}([y]) = \bigsqcup_{y \in [y]} \{t \mid y \in [x](t)\}, \quad (9)$$

and is illustrated by Figure 4.

B. Tube contractor for the constraint $\mathcal{L}_{obs} : y = x(t)$

Sometimes known as *fleeting observation* [3], this constraint $\mathcal{L}_{\text{obs}}$ differs from the ones presented in Section II that apply over the whole trajectory domain. Here, the observation is *local* and leads to an improvement of the estimation of $x(\cdot)$ around t.

In a bounded error context, this constraint is equivalent to:

$$\mathcal{L}_{\text{obs}} : \exists t \in [t], \exists x(\cdot) \in [x](\cdot) \mid x(t) \in [y] \quad (10)$$

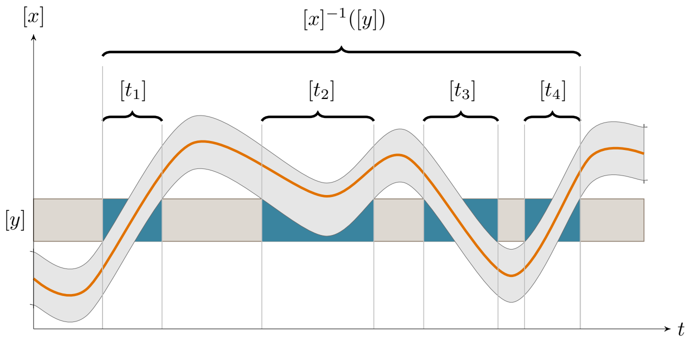

Fig. 4: Tube set-inversion as defined in Equation (9).

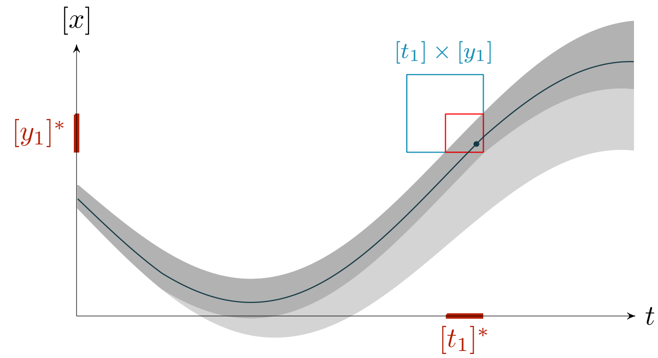

Fig. 5: Observation on a tube $[x](\cdot)$. A given measurement $m_1 \in \mathbb{R}^2$, pictured by a black dot, is known to belong to the blue box $[t_1] \times [y_1]$. The tube is contracted according to Equation (12); the contracted part is depicted in light gray. In the same time, the bounded observation itself can be contracted to $[t_1]^* \times [y_1]^*$ with $[t_1]^* \subseteq [t_1]$ and $[y_1]^* \subseteq [y_1]$. This is illustrated by the red box. The dark line is an example of a trajectory compliant with m_1 that is enclosed within $[t_1]^* \times [y_1]^*$.

Because t is known to belong to an interval $[t]$, it is necessary to consider the evolution of any trajectory of $[x](\cdot)$ along this time interval. Hence the derivative signal $\dot{x}(\cdot)$, that can also be bounded within a tube $[v](\cdot)$[1], is required to apply the constraint $\mathcal{L}_{\text{obs}}$. The consideration of the differential constraint $\dot{x} = v$ is therefore required with $\mathcal{L}_{\text{obs}}$. This information will lead to a propagation of the observation in *forward* and *backward* over the whole trajectory domain. Our problem then amounts to considering the following CSP:

$$\mathcal{L}_{\text{obs}} : \begin{cases} \textbf{Variables: } t,\ y,\ x(\cdot),\ v(\cdot) \\ \textbf{Constraints:} \\ \quad 1)\ \ y = x(t) \\ \quad 2)\ \ \dot{x} = v \\ \textbf{Domains: } [t],\ [y],\ [x](\cdot),\ [v](\cdot) \end{cases} \tag{11}$$

Proposition 3. *A contractor $\mathcal{C}_{obs}\left([t],[y],[x](\cdot),[v](\cdot)\right)$ applying $\mathcal{L}_{\text{obs}}$ on intervals and tubes is defined by:*

$$\begin{pmatrix} [t] \\ [y] \\ [x]\,(t) \\ [v]\,(\cdot) \end{pmatrix} \mapsto \begin{pmatrix} [t] \cap [x]^{-1}([y]) \\ [y] \cap [x]([t]) \\ [x](t) \cap \bigsqcup_{t_1 \in [t]} \left(([x](t_1) \cap [y]) + \int_{t_1}^{t} [v](\tau) d\tau \right) \\ [v]\,(\cdot) \end{pmatrix}. \tag{12}$$

One should note that the tube $[x](\cdot)$ and both $[t]$ and $[y]$ may be contracted while the estimation of the derivative signal, represented by $[v](\cdot)$, will remain the same. Indeed the evolution of any trajectory in $[x]\,(\cdot)$ cannot be known (except for thin tubes). The derivative $\dot{x}(\cdot) \in [v](\cdot)$ can then take any arbitrary value and therefore no information from $[x](\cdot)$ can be propagated back to $[v](\cdot)$.

Proof. To be a contractor, $\mathcal{C}_{\text{obs}}$ needs to satisfy the contraction property (Eq. (4)), but also the completeness (*i.e.* no solution lost, Eq. (5)). The contraction property is trivial as any variable is at least contracted by itself. Thus, it remains to prove that for two real numbers $t \in [t]$, $y \in [y]$ and two signals $x(\cdot) \in [x](\cdot)$, $v(\cdot) \in [v](\cdot)$ such that $y = x(t)$, $\dot{x} = v$, we always have:

$$\begin{pmatrix} t \in [x]^{-1}([y]) & (i) \\ y \in [x]([t]) & (ii) \\ x(\cdot) \in \bigsqcup_{t_1 \in [t]} \left(([x](t_1) \cap [y]) + \int_{t_1}^{t} [v](\tau) d\tau \right) & (iii) \end{pmatrix}.$$

[1] the notation $v(\cdot)$ recalls robot's velocity: the derivative of its position $x(\cdot)$

- (i): since $y \in [y]$, then $x(t) \in [y]$ and thus $t \in x^{-1}([y])$. Assuming $x(\cdot) \in [x](\cdot)$ we have $t \in [x]^{-1}([y])$;
- (ii): since $t \in [t]$, then $y \in x([t])$. Assuming $x(\cdot) \in [x](\cdot)$ we have $y \in [x]([t])$;
- (iii): we assume the observation occurs at t_1: $x(t_1) = y$. Then, based on the set-valued assumptions: $y \in [y] \implies x(t_1) \in [y]$ and $x(\cdot) \in [x](\cdot) \implies x(t_1) \in [x](t_1)$. This implies that $x(t_1) \in ([x](t_1) \cap [y])$. Then, for all t in $x(\cdot)$'s domain, $x(t) = x(t_1) + \int_{t_1}^{t} v(\tau) d\tau$, where $v(\cdot) : \mathbb{R} \to \mathbb{R}$ is the derivative of $x(\cdot)$, enclosed within the tube $[v](\cdot)$. Thus, from the definition of tube integrals [2], $v(\cdot) \in [v](\cdot) \implies \int_{t_1}^{t} v(\tau) d\tau \in \int_{t_1}^{t} [v](\tau) d\tau$, we have $x(t) \in x(t_1) + \int_{t_1}^{t} [v](\tau) d\tau$. Since $x(t_1) \in ([x](t_1) \cap [y])$, $x(t) \in ([x](t_1) \cap [y]) + \int_{t_1}^{t} [v](\tau) d\tau$. This enclosure of $x(t)$ is expressed for a given $t_1 \in [t]$. Therefore the final enclosure of $x(t)$ is provided by: $x(t) \in \bigsqcup_{t_1 \in [t]} \left(([x](t_1) \cap [y]) + \int_{t_1}^{t} [v](\tau) d\tau \right)$.

Remark 4. Extension to multi-dimensional problems $\mathbf{y} = \mathbf{x}(t), \mathbf{y} \in \mathbb{R}^n, \mathbf{x}(\cdot) \in \mathbb{R} \to \mathbb{R}^n$ amounts to apply $\mathcal{L}_{\text{obs}}$ for each component $y_i = x_i(t), i \in \{1 \dots n\}$.

The effect of $\mathcal{C}_{\text{obs}}$ is highlighted in Figure 5 in a non-linear context and strong uncertainties. The derivative $\dot{x}(\cdot)$, not represented here, is also enclosed within a tube.

C. Contractions up to a fixed-point

When dealing with $n \in \mathbb{N}$ observations, a single application of $\mathcal{C}_{\text{obs}}$ for each $[t_i] \times [y_i]$, $i \in \{1..n\}$ may not provide optimal results. Indeed, $\mathcal{C}_{\text{obs}}$ propagates an observation along the whole domain of $[x](\cdot)$ which may lead to new possible contractions. It is preferable to use an iterative method that apply all contractors indefinitely till a fixed point is reached. Figure 6 illustrates the result of $\left(\bigcap_{i=1}^{n} \mathcal{C}_{\text{obs}} \right)^{\infty}$.

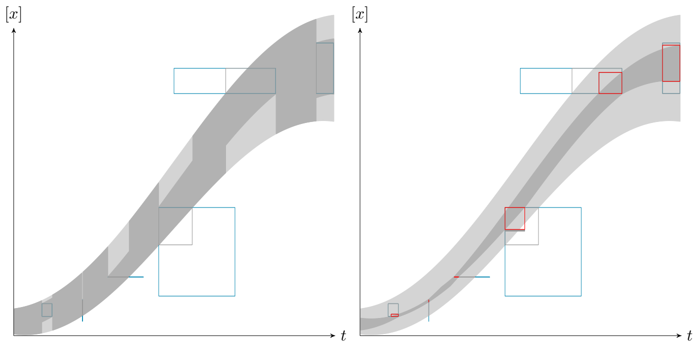

Fig. 6: Combined observation-based contractions on a theoretical example involving a given tube $[x](\cdot)$ and some measurements. The light gray part is the set of trajectories that have been removed after contractions. Blue boxes represent the initial measurements $[t_i] \times [y_i]$. Gray boxes picture intermediate contractions of these observations thanks to the tube. Finally, red boxes depict the minimal contracted measurements $[t_i]^* \times [y_i]^*$.

IV. Range-only Robot Localization with Low-Cost Beacons

The proposed contractor $\mathcal{C}_{\text{obs}}$ will be applied on a state estimation example involving a robot $\mathcal{R}$ moving among several beacons. This application is a simulation based on analytical expressions and simple data in order to encourage future comparisons with the method provided in this paper.

A. Formalization

$\mathcal{R}$ is described by its state $\mathbf{x} = \{x, y\}^\intercal$ depicting its location. The real trajectory taken by the robot is expressed by:

$$\mathbf{x}(t) = \frac{t^2}{2} + 100\begin{pmatrix} -\cos(t) \\ \sin(3t)/3 \end{pmatrix} + \begin{pmatrix} 100 \\ 0 \end{pmatrix}. \tag{13}$$

However, this information is considered unknown. Instead, robot's speed $\mathbf{v} \in \mathbb{R}^2$ is assumed to be known within intervals:

$$\mathbf{v}(t) \in t + 100\begin{pmatrix} \sin(t) \\ \cos(3t) \end{pmatrix} + \begin{pmatrix} [-2,2] \\ [-2,2] \end{pmatrix}. \tag{14}$$

$\mathcal{R}$ evolves among low-cost beacons $\mathbf{b}_k, k \in \mathbb{N}$, thus implying drifting clocks (strong temporal uncertainties) and measurement errors. Then the state estimation problem stands on the following state equations:

$$\left\{ \begin{array}{rcl} \dot{\mathbf{x}}(t) & = & \mathbf{v}(t), \\ y_i(t_i) & = & g_k(\mathbf{x}(t_i)). \end{array} \right. \tag{15}$$

As explained in the introduction of this paper, the first equation depicts the evolution of the system given by Equation (14). The second one provides range-only observations coming from beacons $\mathbf{b}_k$, with a maximum range $\rho_{\max} = 21m$, emitting bounded signals $y_i(t_i), y_i \in [y_i]$ on a regular basis with time uncertainties: $t_i \in [t_i]$. This will highlight the use of $\mathcal{C}_{\text{obs}}$ by providing a set of fleeting bounded measurements to study; see Table II.

k	$\mathbf{b}_k$
1	$(60, 50)$
2	$(35, -5)$
3	$(165, 10)$

TABLE I: Beacons locations.

Range functions are enclosed within tubes $[g_k](\cdot)$ that will be contracted by $\mathcal{C}_{\text{obs}}$. The derivative tube $[\dot{g}_k](\cdot)$ is therefore required for the first contractor:

$$\begin{array}{rcl} [g_k](\cdot) & = & \sqrt{([x_1](\cdot) - b_{k,1})^2 + ([x_2](\cdot) - b_{k,2})^2}, \\ [\dot{g}_k](\cdot) & = & \dfrac{([x_1](\cdot) - b_{k,1}) \cdot [\dot{x_1}](\cdot) + ([x_2](\cdot) - b_{k,2}) \cdot [\dot{x_2}](\cdot)}{\sqrt{([x_1](\cdot) - b_{k,1})^2 + ([x_2](\cdot) - b_{k,2})^2}}. \end{array} \tag{16}$$

The problem amounts to the following CSP. The localization of the mobile robot will be done based on the beacons measurements and without any prior knowledge on initial conditions.

Variables: $\mathbf{x}(\cdot)$, $\mathbf{v}(\cdot)$, $\{g_k(\cdot)\}$, $\{(t_i, y_i)\}$

Constraints:

1) Evolution:
   $\dot{\mathbf{x}}(t) = \mathbf{v}(t)$
2) Range functions:
   $g_k(t) = \sqrt{(x_1(t) - b_{k,1})^2 + (x_2(t) - b_{k,2})^2}$
3) Fleeting observations:
   $y_i = g_k(t_i)$

Domains:
$[\mathbf{x}](\cdot)$, $[\mathbf{v}](\cdot)$, $\{[g_k](\cdot)\}$, $\{([t_i], [y_i])\}$

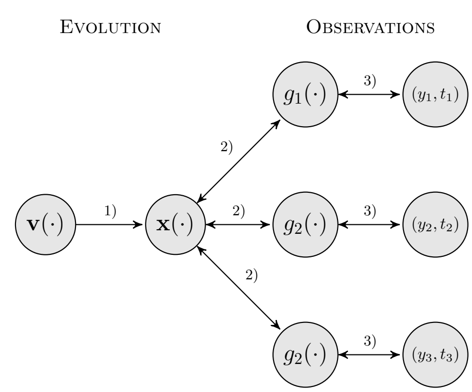

Fig. 7: Constraint network as defined in the CSP, detailing two beacons and three measurements. Arrows indicate the possible directions of propagation of the information. For ease of understanding, derivatives $\dot{g}_k(\cdot)$ are not represented here but are still required for the third constraint. Any improvement on $[\mathbf{x}](\cdot)$ has to be propagated to the $[\dot{g}_k](\cdot)$.

B. Resolution

Constraints defined in the CSP form a constraint network pictured in Fig. 7. Constraints are implemented thanks to contractors applied over intervals and tubes. Tubes are initialized by $[-\infty, \infty], \forall t$.

i	k	$[t_i]$	$[y_i]$
1	2	$[0.88, 0.94]$	$[19.45, 20.45]$
2	3	$[2.04, 2.10]$	$[13.71, 14.71]$
3	3	$[4.14, 4.20]$	$[06.69, 07.69]$
4	2	$[5.38, 5.44]$	$[16.10, 17.10]$
5	2	$[5.68, 5.74]$	$[11.26, 12.26]$
6	2	$[5.98, 6.04]$	$[12.67, 13.67]$
7	1	$[6.89, 6.95]$	$[18.24, 19.24]$
8	1	$[7.19, 7.25]$	$[11.90, 12.90]$

TABLE II: List of measurements $[y_i]([t_i])$.

1) tube $[\mathbf{v}](\cdot)$ is built with tube arithmetic, based on Equation (14). The computation of the envelope of feasible trajectories $[\mathbf{x}](\cdot)$ is then performed thanks to the differential contractor $\mathcal{C}_{\frac{d}{dt}}([\mathbf{x}](\cdot), [\mathbf{v}](\cdot))$ defined in Section II-B;
2) the k-th range tube $[g_k](\cdot)$ is obtained by combining primitive arithmetic tube contractors such as $\mathcal{C}_{\sqrt{\cdots}}$ or $\mathcal{C}_{+}$. The same apply for the k-th derivative range tube;
3) fleeting measurements are applied on $[g_k](\cdot)$. The tube is locally contracted by $\mathcal{C}_{\text{obs}}([t_i], [y_i], [g_k](\cdot), [\dot{g}_k](\cdot))$. The second constraint is then called in order to propagate the measurement back to $[\mathbf{x}](\cdot)$. The first constraint can also apply again to smooth the estimation over the whole domain of $[\mathbf{x}](\cdot)$.

Computed results are pictured in Figure 8.

Remark 5. Dependencies between variables necessarily lead to an iterative resolution process. Furthermore, contractors can be applied regardless of the constraints order and as often as necessary, up to a fixed point.

V. Reliable Correction of a Drifting Clock

A complementary illustration of this work is the case of a drifting clock: an isolated clock that does not run at the same rate as a reference clock. This problem amounts to increasing time uncertainties that can be reduced using a collaborative method [7]. Here, the problem is constrained thanks to a localized robot evolving at the surface and measured distances between the robot and the underwater clock.

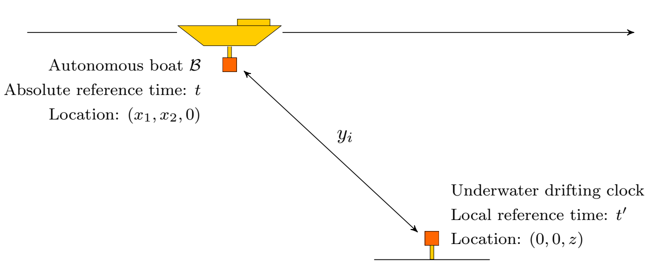

Fig. 9: Illustrating the problem of a drifting clock, corrected by ephemerides provided by an autonomous boat. The beacon holding the clock receives distance measurements from the boat once in a while.

A. Formalization.

Let us take the example of an underwater system, leaned on the seabed at $(x = 0, y = 0, z = -10)$ and equipped with a low-cost clock. Absolute time reference is represented by t

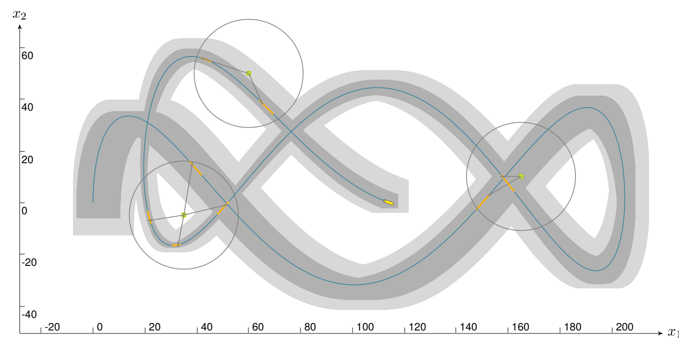

(a) Global map view.

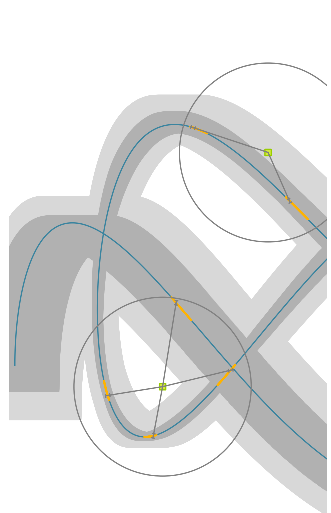

(b) Zoom on beacons $\mathbf{b}_1$ and $\mathbf{b}_2$.

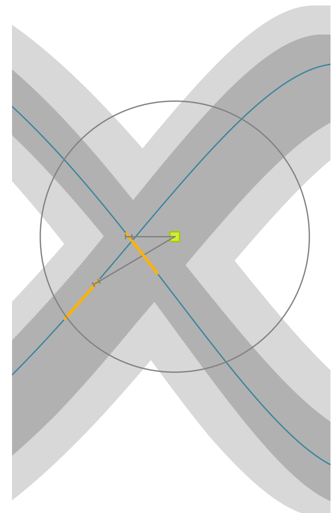

(c) Zoom on beacon $\mathbf{b}_3$.

Fig. 8: State estimation of a mobile robot among a set of beacons, as detailed in Section IV. Initial conditions are not known. Beacons, pictured by green boxes, are sending signals till a range limit drawn by circles. Time uncertainties $[t_i]$ are projected along the robot path with orange thick lines. The true poses of the robot are pictured by the blue line, enclosed within the estimated tubes $[x_1](\cdot) \times [x_2](\cdot)$ projected in gray. The pessimism induced by time uncertainties is represented in light gray. In other words, the dark gray part depicts a state estimation assuming a precise knowledge on the t_i's.

while the time value t' provided by the underwater clock is drifting such that:

$$t' = h(t) = 0.045 \cdot t^2 + 0.98 \cdot t. \tag{17}$$

However, this information is not known. Instead we shall assume the following bounded derivative of $h(\cdot)$, that could be obtained thanks to the clock datasheet:

$$\dot{h}(t) \in [0.08, 0.12] \cdot t + [0.97, 1.08]. \tag{18}$$

The underwater beacon is able to measure distances $y_i \in \mathbb{R}$ from an autonomous boat $\mathcal{B}$ evolving above the clock at the surface, see Figure 9. Boat's trajectory $\mathbf{x}(t) : \mathbb{R} \to \mathbb{R}^2$ is preprogrammed, forming a kind of ephemeris for the clock in the same way as stars have been used for celestial navigation on Earth. This way, the beacon already knows where the robot must be at time t. Conversely, detecting the location of $\mathcal{B}$ provides a temporal information to be compared with the embedded time value. Hence the boat can be used by the underwater clock to correct this temporal drift.

The problem amounts to the following CSP:

$$\left\{\begin{array}{l}\textbf{Variables: } \{(t'_i, y_i)\},\ \mathbf{x}(\cdot),\ h(\cdot),\ d(\cdot)\\ \textbf{Constraints:}\\ \quad 1)\ \text{Ephemerides (\textit{i.e.} boat locations):}\\ \qquad \mathbf{x}(t) \in \begin{pmatrix}[70,90]\\ [10,30]\end{pmatrix} + 100 \cdot \begin{pmatrix}\cos(t)\\ \sin(t)\end{pmatrix}\\ \quad 2)\ \text{Beacon-boat distance function:}\\ \qquad d(t) = \sqrt{x_1(t)^2 + x_2(t)^2 + z^2}\\ \quad 3)\ \text{Drifting time function:}\\ \qquad t' = h(t) = \int_0^t \dot{h}(\tau)d\tau\\ \quad 4)\ \text{Observations:}\\ \qquad y_i(t'_i) = d(t_i) = d(h^{-1}(t'_i))\\ \textbf{Domains: } \{(t'_i, [y_i])\},\ [\mathbf{x}](\cdot),\ [h](\cdot),\ [d](\cdot)\end{array}\right. \tag{19}$$

Remark 6. The boat may not precisely respect the defined schedule. Hence the ephemeris consists in a tube $[\mathbf{x}](\cdot)$ taking into account the possible error of the boat location.

B. Resolution

The bounded prevision of the distances separating the boat from the beacon can be computed with tube arithmetic, as well as its derivative $[\dot{d}](\cdot)$, required for further computations involving the contractor $\mathcal{C}_{\text{obs}}$. The same apply for $[h](\cdot)$ obtained thanks to the derivative $[\dot{h}](\cdot)$.

$$\begin{array}{rcl}[d](\cdot) & = & \sqrt{[x](\cdot)^2 + [y](\cdot)^2 + z^2},\\ [\dot{d}](\cdot) & = & ([x](\cdot)\cdot[\dot{x}](\cdot) + [y](\cdot)\cdot[\dot{y}](\cdot)) \,/\, \sqrt{[d](\cdot)},\\ [h](t) & = & \int_0^t [\dot{h}](\tau)d\tau.\end{array} \tag{20}$$

The beacon receives bounded measurements $[y_i](t'_i)$, see Table III. Tube inversions on $[h](\cdot)$ provide the corresponding enclosures $[t_i] = [h]^{-1}(t'_i)$ of absolute reference times t_i, see Figure 11. The $[t_i]$ are then used to read the ephemeris and are contracted by:

$$\left([t_i], [y_i], [d](\cdot), [\dot{d}](\cdot)\right) \xrightarrow{\mathcal{C}_{\text{obs}}} \left([t_i], [y_i], [d](\cdot), [\dot{d}](\cdot)\right). \tag{21}$$

Remark 7. The $[y_i]$ and $[d](\cdot)$ are little or not contracted because relatively thin regarding other variables.

Contracted $[t_i]$ can be used to reduce the tube $[h](\cdot)$ using the same contractor:

$$\left([t_i], t'_i, [h](\cdot), [\dot{h}](\cdot)\right) \xrightarrow{\mathcal{C}_{\text{obs}}} \left([t_i], t'_i, [h](\cdot), [\dot{h}](\cdot)\right). \tag{22}$$

Eventually, the contracted tube $[h](\cdot)$ reflects the clock drift correction, see Figure 11. One should note that the real drift $h(t)$ – unknown of the resolution – remains enclosed in its final envelope $[h](t), \forall t$.

An iterative resolution process may be executed up to a fixed point. Indeed, the first contraction of $[h](\cdot)$ (Equation (22)) may raise new constraints for the contraction of the $[t_i]$ (Equation (21)).

i	t'_i	$[y_i]$
1	1.57	$[152.47, 156.47]$
2	3.34	$[34.67, 38.67]$
3	5.32	$[102.38, 106.38]$
4	7.50	$[184.45, 188.45]$
5	9.88	$[167.09, 171.09]$
6	12.46	$[60.03, 64.03]$
7	15.25	$[78.76, 82.76]$
8	18.24	$[175.88, 179.88]$

TABLE III: List of measurements $[y_i](t'_i)$.

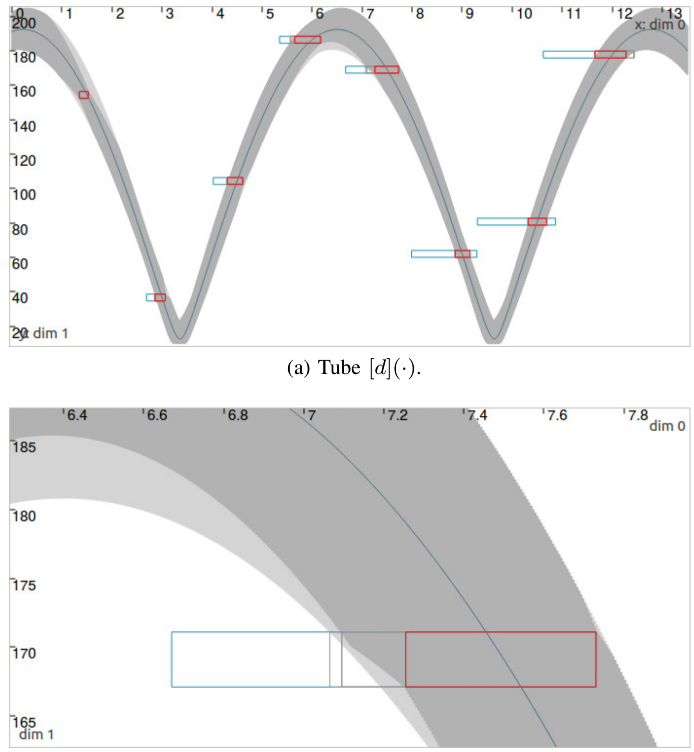

(a) Tube $[d](\cdot)$.

(b) Zoom on tube $[d](\cdot)$.

Fig. 10: Tube $[d](\cdot)$ representing the reliable prevision of the distances between the boat and the beacon (so-called *ephemeris*). $[d](\cdot)$ is submitted to a set of measurements pictured in blue, before their final contraction in red. This demonstrates the contraction of strong time uncertainties thanks to the knowledge provided by the tube itself.

VI. Conclusions

This paper provides an original method to deal with time uncertainties in non-linear and differential systems. The proposed framework, based on tubes depicting envelopes of trajectories, is generic and simple to use. The principle is to model the problem as a constraint network and generate a contractor from each constraint. The tubes containing the variables are then contracted as much as possible. This paper then focuses on the special constraint $y = x(t)$ depicting a trajectory observation at a given moment. The proposed related contractor is then illustrated over two robotics examples in which we show its ease of use. The solutions obtained with the developed framework are guaranteed and can be used for proofs purposes, *e.g.* algorithms validations, path planning and collision avoidance. Future work will focus on real robotics

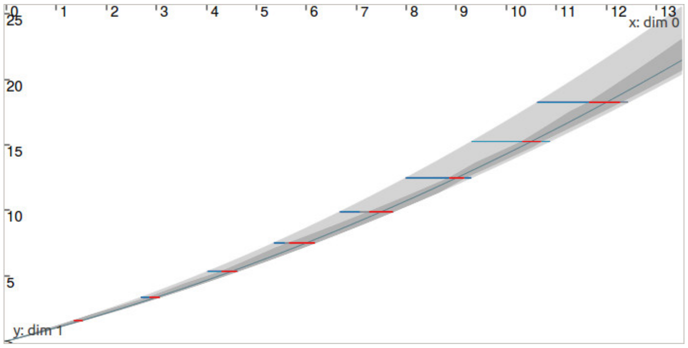

(a) Tube $[h](\cdot)$.

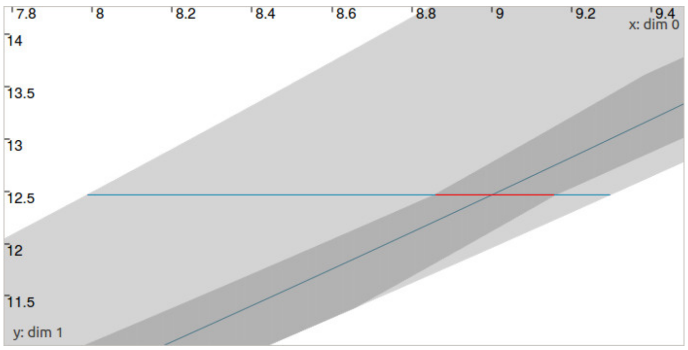

(b) Zoom on tube $[h](\cdot)$.

Fig. 11: Tube $[h](\cdot)$ representing the clock drift. For a given time t', $[h](\cdot)$ provides an enclosure $[t]$ of the time reference t. When $[t]$ is contracted by means of ephemeris $[d](\cdot)$ and $\mathcal{C}_{\text{obs}}$ (see Figure 10), the information can be propagated back to $[h](\cdot)$. Tube's contracted part is pictured in light gray while the real drift expressed by Equation (17) is plotted in blue.

applications involving such uncertainties.

VII. Available Libraries

An optimized tube class has been implemented during this work and is available on: www.simon-rohou.fr/research/tubobs. The source code of the simulated examples presented in this paper are also provided in this library. This class is compatible with IBEX: a C++ library for system solving and global optimization based on interval arithmetic and constraint programming, see www.ibex-lib.org. Figures have been drawn using the visualizer VIBEs [11].

VIII. Acknowledgments

This work has been supported by the French *Direction Générale de l'Armement* (DGA) during the UK-France PhD program.

References

[1] I. Araya, G. Trombettoni, and B. Neveu. A contractor based on convex interval Taylor. In *Proc. of CPAIOR*, pages 1–16, LNCS 7298, Springer, 2012.

[2] C. Aubry, R. Desmare, and L. Jaulin. Loop detection of mobile robots using interval analysis. *Automatica*, 2013.

[3] F. Le Bars, J. Sliwka, O. Reynet, and L. Jaulin. State estimation with fleeting data. *Automatica*, 48(2):381–387, 2012.

[4] C. Bessiere. Constraint propagation. *Foundations of Artificial Intelligence*, 2:29–83, 2006.

[5] A. Bethencourt and L. Jaulin. Cooperative localization of underwater robots with unsynchronized clocks. *Paladyn, Journal of Behavioral Robotics*, 4(4):233–244, 2013.

[6] A. Bethencourt and L. Jaulin. Solving non-linear constraint satisfaction problems involving time-dependant functions. *Mathematics in Computer Science*, 8(3), 2014.

[7] A. Caiti, A. Garulli, F. Livide, and D. Prattichizzo. Localization of autonomous underwater vehicles by floating acoustic buoys: a set-membership approach. *IEEE Journal of Oceanic Engineering*, 30(1):140–152, 2005.

[8] G. Chabert and L. Jaulin. Contractor Programming. *Artificial Intelligence*, 173:1079–1100, 2009.

[9] M. Choi, J. Choi, J. Park, and W. K. Chung. State estimation with delayed measurements considering uncertainty of time delay. In *ICRA*, pages 3987–3992. IEEE, 2009.

[10] C. Combastel. A state bounding observer for uncertain non-linear continuous-time systems based on zonotopes. In *CDC-ECC '05*, 2005.

[11] V. Drevelle and J. Nicola. Vibes: A visualizer for intervals and boxes. *Mathematics in Computer Science*, 8(3-4):563–572, 2014.

[12] A. Gning and P. Bonnifait. Constraints propagation techniques on intervals for a guaranteed localization using redundant data. *Automatica*, 42(7):1167–1175, 2006.

[13] L. Jaulin, M. Kieffer, I. Braems, and E. Walter. Guaranteed nonlinear estimation using constraint propagation on sets. *International Journal of Control*, 74(18):1772–1782, 2001.

[14] L. Jaulin, M. Kieffer, O. Didrit, and E. Walter. *Applied Interval Analysis, with examples in parameter and state estimation, robust control and robotics*. Springer-Verlag, London, 2001.

[15] A. Kurzhanski and I. Valyi. *Ellipsoidal calculus for estimation and control*. Birkhäuser, Boston, MA, 1997.

[16] A. K. Mackworth. Consistency in networks of relations. *Artificial Intelligence*, 8(1):99–118, February 1977.

[17] M. Milanese, J. Norton, H. Piet-Lahanier, and E. Walter, editors. *Bounding Approaches to System Identification*. Plenum Press, New York, NY, 1996.

[18] M. Milanese and A. Vicino. Estimation theory for nonlinear models and set membership uncertainty. *Automatica*, 27(2):403–408, 1991.

[19] R. E. Moore. *Interval Analysis*. Prentice-Hall, Englewood Cliffs, NJ, 1966.

[20] R. E. Moore. *Methods and applications of interval analysis*. SIAM, Philadelphia, PA, 1979.

[21] T. Raissi, N. Ramdani, and Y. Candau. Set membership state and parameter estimation for systems described by nonlinear differential equations. *Automatica*, 40:1771–1777, 2004.

[22] S. Rohou, L. Jaulin, L. Mihaylova, F. Le Bars, and S. M. Veres. Guaranteed computation of robots trajectories,

2016.
[23] P. van Hentenryck, L. Michel, and Y. Deville. *Numerica - a modelling language for global optimization*. MIT Press, Cambridge, Massachusetts, 1997.
[24] S. M. Veres. Error control in polytope computations. *Journal of Optimization Theory and Applications*, 113(2):325–355, 2002.